Circular dichroism measurements at an x-ray free-electron laser with polarization control

G. Hartmann, A. O. Lindahl, , A. Knie, N. Hartmann, , A. A. Lutman, J. P. MacArthur, I. Shevchuk, J. Buck, A. Galler, J. M. Glownia, W. Helml, , Z. Huang, N. M. Kabachnik, , A. K. Kazansky, , J. Liu, A. Marinelli, T. Mazza, H.-D. Nuhn, P. Walter, J. Viefhaus, M. Meyer, S. Moeller, R. N. Coffee, and M. Ilchen,

Circular dichroism measurements at an x-ray free-electron laser with polarization control

G. Hartmann,[1] A. O. Lindahl,[2,a)] A. Knie,[3] N. Hartmann,[4,b)] A. A. Lutman,[4] J. P. MacArthur,[4] I. Shevchuk,[1] J. Buck,[5] A. Galler,[5] J. M. Glownia,[4] W. Helml,[4,c)] Z. Huang,[4] N. M. Kabachnik,[6,d)] A. K. Kazansky,[7,e)] J. Liu,[5] A. Marinelli,[4] T. Mazza,[5] H.-D. Nuhn,[4] P. Walter,[1] J. Viefhaus,[1] M. Meyer,[5] S. Moeller,[4] R. N. Coffee,[4] and M. Ilchen[4,f)]

[1]Deutsches Elektronen-Synchrotron, Notkestraße 85, 22607 Hamburg, Germany
[2]PULSE at Stanford, 2575 Sand Hill Road, Menlo Park, California 94025, USA
[3]Institut für Physik, University of Kassel, Heinrich-Plett-Str. 40, 34132 Kassel, Germany
[4]SLAC National Accelerator Laboratory, 2575 Sand Hill Road, Menlo Park, California 94025, USA
[5]European XFEL GmbH, Albert-Einstein-Ring 19, 22761 Hamburg, Germany
[6]Skobeltsyn Institute of Nuclear Physics, Lomonosov Moscow State University, Moscow 119991, Russia
[7]Departamento de Fisica de Materiales, UPV/EHU, Donostia International Physics Center (DIPC), E-20018 San Sebastian/Donostia, Spain

A non-destructive diagnostic method for the characterization of circularly polarized, ultraintense, short wavelength free-electron laser (FEL) light is presented. The recently installed Delta undulator at the LCLS (Linac Coherent Light Source) at SLAC National Accelerator Laboratory (USA) was used as showcase for this diagnostic scheme. By applying a combined two-color, multi-photon experiment with polarization control, the degree of circular polarization of the Delta undulator has been determined. Towards this goal, an oriented electronic state in the continuum was created by non-resonant ionization of the O_2 1s core shell with circularly polarized FEL pulses at $h\nu \simeq 700$ eV. An also circularly polarized, highly intense UV laser pulse with $h\nu \simeq 3.1$ eV was temporally and spatially overlapped, causing the photoelectrons to redistribute into so-called sidebands that are energetically separated by the photon energy of the UV laser. By determining the circular dichroism of these redistributed electrons using angle resolving electron spectroscopy and modeling the results with the strong-field approximation, this scheme allows to unambiguously determine the absolute degree of circular polarization of any pulsed, ultraintense XUV or X-ray laser source. *Published by AIP Publishing.* [http://dx.doi.org/10.1063/1.4961470]

I. INTRODUCTION

Free-electron lasers (FELs) with their ultrashort and ultraintense pulses ranging from the InfraRed (IR) over the Vacuum UltraViolet (VUV) to the hard X-ray regime have revolutionized the field of photon science.[1] One key development at the LCLS, at SLAC, USA towards new applications with X-ray free-electron lasers (XFELs) is the "*Delta*" project[2,3] that preludes their capability to provide circularly polarized X-rays with a very high degree of circular polarization while preserving characteristics unique to FELs such as high pulse energies and ultrashort pulses.

Generally, circularly polarized light enables investigations on all chiral, i.e., optically active targets. The difference in the absorption coefficients of left-handed light and right-handed light of a chiral target is called "*circular dichroism*." Dichroic behavior of matter has wide applications in studies of magnetism,[4] data storage,[5] spintronics,[6] and biological chirality of any living tissue on earth[7] due to its sensitivity for electronic spin and structural chirality of, e.g., biomolecules. Regarding its impact on our health and well-being, the pharmaceutical industry invests billions of dollars each year in drug control and discovery where chirality can determine the benefit versus toxicity of a compound.[8]

Already with the advent of circularly polarized FEL light in the VUV regime at FERMI (Free Electron laser Radiation for Multidisciplinary Investigations) in Italy,[9–12] e.g., ultrafast changes of magnetism gained broad interest over the last years[13–15] and will also be one of the main applications for the Delta undulator. Not only techniques using ultrafast X-rays and optical lasers[13–15] but also the use of transient spin gratings,[16] the time resolved magneto-optical Kerr effect,[17] and ultrafast electron diffraction (UED) experiments[18] has shown

---

a)Also at University of Gothenburg, SE-412 96 Gothenburg, Sweden.
b)Also at University of Bern, Sidlerstraße 5, CH-3012 Bern, Switzerland.
c)Also at Technical University of Munich, James-Franck-Straße 1, 85748 Garching, Germany.
d)European XFEL GmbH, Albert Einstein Ring 19, 22761 Hamburg, Germany and Departamento de Fisica de Materiales, UPV/EHU, Donostia International Physics Center (DIPC), E-20018 San Sebastian/Donostia, Spain.
e)IKERBASQUE, Basque Foundation for Science, E-48011 Bilbao, Spain.
f)Author to whom correspondence should be addressed. Electronic mail: markus.ilchen@xfel.eu. Also at PULSE at Stanford, 2575 Sand Hill Road, Menlo Park, California 94025, USA and European XFEL GmbH, Albert-Einstein-Ring 19, 22761 Hamburg, Germany.

great potential to contribute to the scientific field of ultrafast magnetism studies. UED is anticipated to also contribute to the study of ultrafast structural changes of chiral molecules and constitutes a promising synergy between XFEL research and electron diffraction.

With the advent of ultrafast, highly intense, and chiral X-rays at even higher photon energies, the understanding of underlying processes in large material depth or involving highly bound electrons can be studied in advanced detail on a femtosecond time scale. Furthermore, spin control in non-linear physics of, e.g., sequential photoionization,[19] as well as transient core shell chirality studies of bio-molecules[20] will be enabled by the Delta undulator.

Previous efforts to generate ultrafast chiral X-rays were performed with an in-plane-magnetized Co magnetic thin film polarizer[13] at the LCLS at 778 eV. This approach resulted in 10^9 photons per pulse ($\approx$120% nJ pulse energy) with 58% of circular polarization.

Sliced synchrotron radiation sources[21] as another promising technique to study ultrafast chiral and magnetic dynamics have demonstrated to provide a higher degree of circular polarization in ultrashort X-ray pulses but are limited in their pulse energies and their peak power as well.

Compared to these approaches and any ultrafast, circularly polarized optical or higher harmonic generation laser, the Delta operation at LCLS can produce a very high degree of circular polarization and, at the same time, orders of magnitude higher pulse energies of tens to hundreds of μJ X-ray pulse energy. The typical pulse durations range from 10 fs to 40 fs.

For circularly polarized hard X-rays as a future perspective, an even deeper penetration depth and the site selectivity for several magnetic as well as paramagnetic materials[23] are of interest with future applications towards ultrafast investigations as well. Details about Delta, its general operation and the advanced modes are published elsewhere.[22]

In this work, we present direct measurements of the degree of circular polarization of the X-ray pulses generated by the Delta undulator. The chosen photon energy is a showcase for the performance of Delta and is particularly interesting for future experiments on chiral molecular structures that contain atoms such as fluorine as well as for X-ray Magnetic Circular Dichroism (XMCD) studies at several M- and L-edges of magnetic elements. Based on these results, an online polarization diagnostic scheme has been calibrated and used for further commissioning.

II. EXPERIMENT

The experiment was based on a two-color, multi-photon, and variable polarization interaction with K-shell electrons of molecular oxygen. By ionizing oxygen core electrons ($E_{Bind} \approx 540$ eV) with a circularly polarized (and therefore chiral) FEL pulse of $h\nu = 700$ eV, chiral electronic states were created in the continuum. These O_2 1s photoelectrons were emitted in the strong field of a spatially and temporally overlapped, circularly polarized, UV laser with 3.1 eV photon energy. This laser field redistributed the electrons in additional peaks, the sidebands, that are separated by the energy of the laser photons.

Depending on the chirality of the Delta-light, the yields of the sidebands differ substantially, see Fig. 2, which allows a quantitative analysis of the underlying degree of circular polarization within a model based on the strong field approximation[24,25] (see the supplementary material for details of the theoretical modeling).

For the work presented here, previous polarization diagnostics[12] have been substantially developed in order to meet the demands of an X-ray SASE (Self Amplified Stimulated Emission) light source like the LCLS. To enable the measurement of photoelectron sidebands in the X-ray regime, an angle resolving electron time-of-flight spectrometer was installed in the Atomic, Molecular and Optical Sciences beamline of the LCLS.[26] The spectrometer made it possible to measure electron kinetic energies of several hundreds and potentially thousands of electronvolts. To account for the typically large SASE energy bandwidth and the resulting energy broadening of the electron signal, we used a frequency doubled Ti:Sapphire laser providing ultraviolet (UV) light with 400 nm wavelength (3.1 eV photon energy). Furthermore, the data was sorted and filtered to include only those X-ray pulses with small bandwidth and good overlap with the UV light. The details of the data processing are described below.

For the X-ray generation, 11 planar (linearly polarizing) LCLS undulators were used to create a micro-bunched electron beam with 3.97 GeV kinetic energy at the full repetition rate of the LCLS, 120 Hz. The electron beam was then sent through the 3.2 m Delta undulator in left or right circular polarization mode. To extract maximal X-ray intensity from an electron bunch, the magnetic field strength is commonly reduced along the planar undulator line, a so called normal taper. A reversed taper, on the other hand, increases the field strength along the undulator line, which suppresses lasing but still produces microbunching.[22,27,28]

The total average pulse energy was determined to be 16 μJ with a FWHM of 4.5 μJ for the reversed taper operation and 81 μJ with a FWHM of 28 μJ for the normal taper operation. The pulse duration of 80 fs ± 20 fs with a jitter of 100 fs RMS was the same for both taper conditions. The post-sorting of the temporal jitter is principally possible at the LCLS with different arrival time techniques.[29–31] However, under the described conditions of the experiment the X-ray intensity was insufficient for such techniques. Instead, a data sorting as described below was applied to remedy the temporal jitter uncertainty. An energy jitter of the X-ray photon energy of ±2.5 eV was determined and sorted in the analysis based on measurements of the electron beam energy as provided by the facility. The average bandwidth including all shots and data sets was ≈4 eV. Any residual energy jitter is included in the final bandwidth determination. The X-rays were focused down to a spot with 20 ± 10 μm diameter at FWHM in the interaction region.

The UV light was produced by second harmonic generation of 800 nm radiation from a standard Ti:Sapphire laser system in a Beta Barium Borate (BBO) crystal. Three reflections on dichroic mirrors were used to remove any residual 800 nm radiation before the 400 nm light was focused by a curved mirror into the interaction region. The laser was more than 99% circularly polarized by a zero order quarter waveplate.

The spot size of the UV radiation was 100 ± 15 μm at FWHM and the pulse energy was 234 ± 10 μJ. A pulse duration of 50 ± 10 fs of the UV light and a timing jitter of 120 fs RMS made event filtering essential to analyze shots with good time overlap. After establishing a coarse time overlap of the UV laser and the FEL with a diode signal ($\approx$20 ps accuracy), the sideband generation was subsequently used to determine the best time overlap between the X-ray and UV pulses.

Regarding the sample, gaseous oxygen with a purity of 99.995% was injected into the interaction region of an ultra-high vacuum chamber via an effusive gas jet. The background pressure in the experimental chamber was in the order of 1×10^{-9} hPa. The maximum pressure with injected oxygen was kept below 10^{-5} hPa to ensure proper operation of the detectors.

For the detection of the chirally distributed electrons emitted from the oxygen, an array of 16 independently working time-of-flight spectrometers was used. The detectors were arranged in the plane perpendicular to the light propagation[11,32] (see Fig. 1). Details about the technical specifications of the spectrometer will be published elsewhere.

III. RESULTS AND DISCUSSION

A total of 60 min of data was recorded in four 15 min data sets for combinations of both helicities of the X-rays and the normal and reversed taper conditions. The first step of the analysis was to determine a conversion between the time-of-flight of the electrons and their energy. This was achieved by analyzing dedicated calibration measurements where the X-ray energy was changed in few-eV steps around the nominal energy. The relative transmission and gain factors of the different detectors were determined by analyzing non-resonant Auger electron signals known to be inherently isotropic. In this way, the electron spectra could be converted to an absolute energy axis with correct relative intensities.

As a first step of polarization determination, the degree of linear polarization was derived from the total intensity of each detector as a function of the emission angle θ in the plane of the light polarization vector. The resulting electron angular distribution in this plane can be described in terms of the degree of linear polarization in the sense of the first Stoke's parameter P_1 as

$$\frac{d\sigma_{if}}{d\Omega}(\theta) = \frac{\sigma_{if}}{4\pi}\left[1 + \frac{\beta_{if}}{4}\left(1 + 3P_1 \cos\left[2(\theta - \lambda)\right]\right)\right], \quad (1)$$

with the anisotropy parameter β_{if} and the cross section σ_{if} from the initial to the final electronic state.[33] The tilt angle λ characterizes the axis of the linear polarization where $\lambda = 0$ represents horizontal polarization. The β_{if}-parameter for non-resonant photoelectron emission from the O$_2$ 1s orbitals is very close to 2 for the kinetic energy of 156 eV. The approximation of a maximum anisotropy ($\beta = 2$) and a pure p-wave emission is generally valid for fast electrons emitted from highly localized isotropic orbitals ionized by horizontally polarized photons since the by far dominant emission direction is determined by the polarization vector. This means that for horizontally polarized light as emitted from planar undulator segments, the O$_2$ 1s electrons are emitted along the horizontal axis. In that case, the largest signal is detected in the $\theta = 0°$ and $\theta = 180°$ detectors (see Fig. 1) whereas the detectors at $\theta = 90°$ and $\theta = 270°$ show no signal for the O$_2$ 1s electrons. For the case of circular polarization as emitted from the Delta undulator, the O$_2$ 1s electrons are emitted isotropically where every detector must measure the same spectrum. Both extreme cases are depicted as "3D emission patterns" above their respective sources in Fig. 1. The overlap of linear and circular polarization causes an elliptical distribution which still unambiguously allows the derivation of the linear polarization component. This method can, however, not distinguish between circularly and unpolarized light, which is the main motivation for using a circular dichroism as the unambiguous measure of the circular polarization.

Using Eq. (1), the degree of linear polarization was determined to be $P_{1,\text{(Reversed taper)}} = 0.05(3)$ for the reversed taper and $P_{1,\text{(Normal taper)}} = 0.25(2)$ for normal taper. Using a common expression for the degree of total polarization, $p^2 = P_1^2 + CP^2$,[11] these values correspond to a fraction of non-linearly polarized light of 96.8(5)% for the normal taper and 99.9(1)%
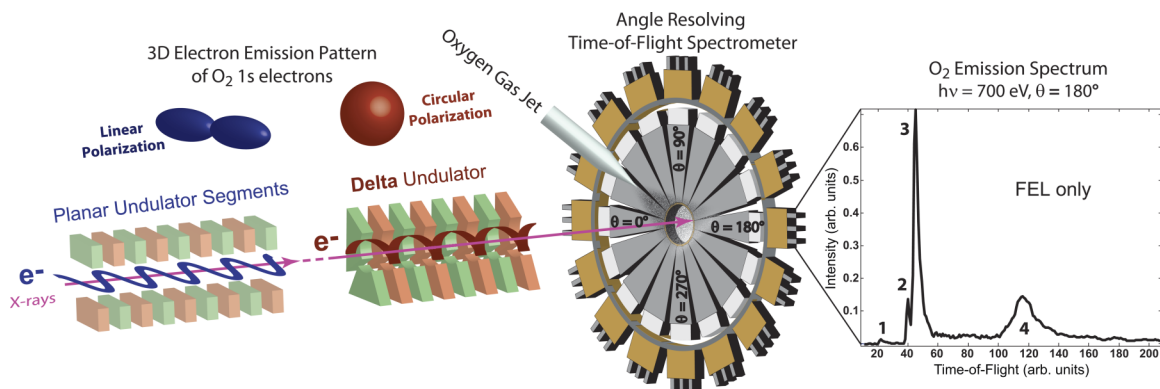
FIG. 1. Experimental scheme figuring the X-ray generation in the planar undulator segments and in the Delta undulator (only two of the magnet rows are depicted) as well as the experimental setup consisting of 16 independently working time-of-flight (TOF) spectrometers aligned in the plane of polarization under the angle θ (see Eq. (1)). The angular distribution patterns above the respective undulator sections depict the emission from linearly (horizontally) polarized and the circularly polarized light. The spectrum on the right shows a schematic "FEL only" O$_2$ time-of-flight spectrum at 700 eV photon energy under the $\theta = 180°$ emission angle. Here, 1 marks the scattered light, 2 are valence electrons, 3 are Auger electrons and 4 are O$_2$ 1s electrons which can be redistributed in the sidebands by overlapping the UV laser with the X-ray pulse.

for the reversed taper. These results are robust and independent of any selection or filtering of the data. Therefore, this is a strong indication that the general polarization stability of Delta was good throughout the measurements.

Before analyzing the degrees of circular polarization, the data had to be filtered based on two criteria. The first selection was made based on the bandwidth of the X-rays. This was achieved by determining the width of the main photo-line for each FEL shot. Only shots where the FEL bandwidth was less than 2.5 eV (≈7% of the total) were used in the further analysis. The second selection was based on the total sideband intensity relative to the main line, which was acquired from an intensity fit on the respective contributions in each shot (≈30% of the first step filtering). Accordingly, a total of about 2% of the incoming FEL shots was used for the final analysis. This filtering served the purpose of disregarding shots where either the temporal or spatial overlap was compromised due to temporal jitter or pointing instabilities. The polarization jitter itself is estimated to be very low by observing the shot-to-shot fluctuations of the degree of linear polarization. The residual uncertainty is taken into account in the final error. Selecting only the strongest sideband signals can be justified since the modeling was based on the best overlap condition. This selection was furthermore checked to only provide signals with the same absolute FEL intensity in order to ensure the validity of the used modeling.[24,25]

Including shots where the temporal or spatial overlaps were sub-optimal would lead to an underestimation of the circular dichroism and thus the degree of circular polarization.

In order to directly determine the degree of circular polarization, the difference between spectra derived from left and

right circularly polarized X-rays, as shown in Figure 2(a), was correlated to the theoretical calculations (see Figure 2(b). A benefit of the subtraction is an improvement of the data representation because all detector related behavior such as ringing, cross talk, and individual electron transmission is intrinsically eliminated. For this part of the study, the emission angle was not of importance and the spectra from all 16 detectors were averaged for better statistics. The theoretical modeling is described in detail in papers[24,25] and was previously applied for the description of sideband spectra,[34] angular distribution of photoelectrons,[35] and circular dichroism in sidebands.[12] It can be found in the supplementary material for further reading.

From four data sets, reversed taper with left circular polarization and normal taper with right circular polarization have superior statistical quality compared to the opposite polarizations of the corresponding taper modes. The reason for this circumstance is probably related to small drifts in the overlap conditions of the UV laser and the FEL. Although the changing taper is expected to deliver slightly different polarization characteristics, within the used model, it is still valid to simply determine the average degree of polarization between the two helicities.[24,25]

Fig. 2(a) shows the energy converted sideband spectra for left and right circularly polarized light which were sorted for sufficiently low bandwidth and the same overlap conditions with the UV laser as described above. The energy shift between the center of gravity of the two spectra towards higher kinetic energies is caused by slightly different energy and polarization conditions in the two taper modes as characterized above. In order to achieve the most reliable results, the spectra are focused on the high kinetic energy side of the sidebands and in particular the ratio between main line and the first sideband in the difference spectrum due to statistical reasons. However, all sidebands and their respective contributions have been taken into account for the determination of the results. The error bars as shown in Figure 2(b) include the statistical error, the background correction, and the transmission correction, all derived by Gaussian error progression. Due to low spectrometer transmission and therefore less favorable statistics for sidebands with negative relative kinetic energies, the corresponding data is not included. The difference of these spectra is shown as data points connected with a full red line in Fig. 2(b) (reversed taper left circular vs. normal taper right circular), while the difference spectra involving the lower quality data sets are combined to points representing the mainline and two visible sidebands. These points have increased uncertainties but the results are qualitatively consistent with the reversed vs. normal taper comparison. The statistics for the second sideband for the reversed taper are low and therefore not shown. The theoretical result with the matching electron kinetic energy of 156 eV is depicted as a full blue line in the figure. This kinetic energy has been determined experimentally and has an error of less than 2 eV. The bandwidth of the theoretical data has been chosen to match the experimentally sorted bandwidth of 2.5 eV FWHM. For a guide-to-the-eye comparison, calculations for 150 eV electron kinetic energy as a lower relevant limit and 171 eV electron kinetic energy as an upper relevant limit are shown as full gray lines. It is interesting to point out that the changes in sideband yields between the
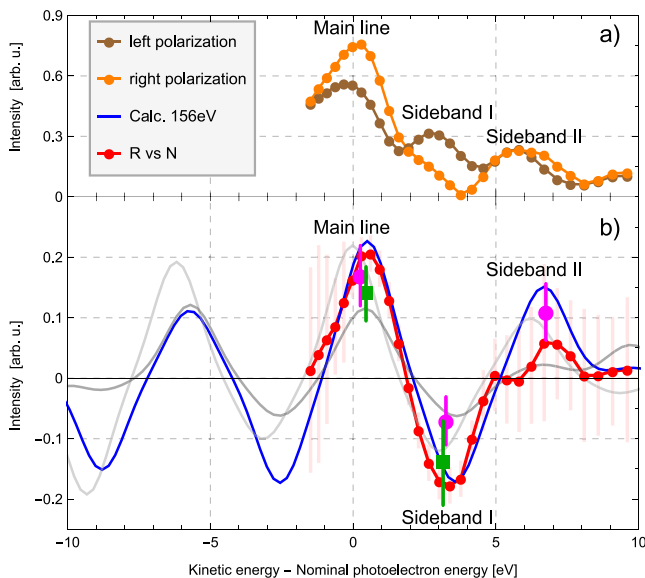
FIG. 2. Figure 2(a) depicts the energy calibrated, angle integrated O_2 1s spectra for left and right circular polarization of Delta with overlapped UV laser. Figure 2(b) shows the difference of these spectra (connected red dots) as well as the according calculations for 156 eV kinetic energy (blue line) and supporting experimental results from specific tapers (magenta circles: normal; green squares: reversed). Also shown are calculations for the difference spectra at electron kinetic energies in the vicinity of the experimental data (lighter gray: 150 eV; darker gray: 171 eV).

different curves as predicted by theory are quite big regarding the rather large absolute kinetic energies. This implies that the kinetic electron energy is a sensitive parameter for this method which has been taken into account for the total error of the degree of circular polarization.

The difference spectrum from the left circular reversed taper and the right circular normal taper was used in a comparison to the theoretical modeling and the average degree of circular polarization was determined to be CP = 92% ± 6%. Given that the polarized part of the beam, p, is commonly written to be $p^2 = P_1^2 + CP^2$,[11] the unpolarized part is assumed to be constant, the degrees of linear polarization for the two taper modes are $P_{1,(\text{Reverse taper})} = 0.05(3)$ and $P_{1,(\text{Normal taper})} = 0.25(2)$, and the degrees of circular polarization were determined to be 95% $^{+5\%}_{-6\%}$ for reversed taper and 89% ± 6% for normal taper.

Within the accuracy of the measurements there was no change in any degree of polarization upon switching the beam helicity within a specific taper mode. Especially the very accurately measurable degree of linear polarization validates the expectation of a stable degree of polarization during helicity changing.

All variably polarized components that are undetectable for our method are combined to represent the "unpolarized" part of the FEL beam which according to the above numbers adds up to 5% $^{+6\%}_{-5\%}$ for both taper modes.

IV. CONCLUSION

In conclusion, we have measured a circular dichroism with the Delta undulator and determined the degree of circular polarization to be 95% $^{+5\%}_{-6\%}$ for reversed taper and 89% ± 6% for normal taper under the described conditions. We exploited the creation of chiral electronic states in the continuum in molecular inner-shell ionization of oxygen with circularly polarized X-rays using a SASE based XFEL and a second harmonic UV laser. The experimental scheme of using a second harmonic optical laser with angle resolving electron time-of-flight spectroscopy and specifically developed data analysis as presented here enables this kind of diagnostic to be applicable to any kind of SASE based X-ray source.

The operation of the Delta undulator is under ongoing development and schemes to improve the absolute degree of circular polarization are explored and will be published subsequently. The presented data have been analyzed for a single shot determination of the degree of circular polarization which in principal works, however facing too low single shot statistics for a quantitative analysis. It is anticipated to be feasible in the near future. Furthermore, it would be interesting to investigate the SASE sub-structure of the FEL pulses with, e.g., electron streaking techniques for their individual polarizations. Future projects on the exploration of chirality, magnetization studies, and general spin control are also under ways. The data presented here support the prospected capabilities of future FEL projects like European XFEL and the LCLS II to promote and include polarization control as a top priority together with robust diagnostics.

SUPPLEMENTARY MATERIAL

See supplementary material for further reading about the theoretical modeling of dichroic behavior of a laser dressed electron in the continuum after FEL ionization.

[1]P. Emma, R. Akre, J. Arthur, R. Bionta, C. Bostedt, J. Bozek, A. Brachmann, P. Bucksbaum, R. Coffee, F.-J. Decker *et al.*, Nat. Photonics **4**, 641–647 (2010).

[2]H.-D. Nuhn, S. Anderson, G. Bowden, Y. Ding, G. Gassner, Z. Huang, E. M. Kraft, Y. Levashov, F. Peters, F. E. Reese *et al.*, SLAC-PUB, 15743, 2014.

[3]A. B. Temnykh, Phys. Rev. Spec. Top.–Accel. Beams **11**, 120702 (2008).

[4]C. Boeglin, E. Beaurepaire, V. Halte, V. Lopez-Flores, C. Stamm, N. Pontius, H. A. Dürr, and J. Y. Bigot, Nature **465**, 7297 (2010).

[5]C. Chappert, A. Fert, F. Nguyen, and V. Dau, Nat. Mater. **6**, 813–823 (2007).

[6]M. Mannini, F. Pineider, P. Sainctavit, C. Danieli, E. Otero, C. Sciancalepore, A. M. Talarico, M. A. Arrio, A. Cornia, D. Gatteschi, and R. Sessoli, Nat. Mater. **8**, 194–197 (2009).

[7]J. S. Siegel, Chirality **10**, 24 (1998).

[8]L. A. Nguyen, H. He, and C. Pham-Huy, Int. J. Biomed. Sci. **2**, 85–100 (2006).

[9]C. Spezzani, E. Allaria, M. Coreno, B. Diviacco, E. Ferrari, G. Geloni, E. Karantzoulis, B. Mahieu, M. Vento, and G. De Ninno, Phys. Rev. Lett. **107**, 084801 (2011).

[10]E. Allaria, R. Appio, L. Badano, W. A. Barletta, S. Bassanese, S. G. Biedron, A. Borga, E. Busetto, D. Castronovo, P. Cinquegrana *et al.*, Nat. Photonics **6**, 699 (2012).

[11]E. Allaria, B. Diviacco, C. Callegari, P. Finetti, B. Mahieu, J. Viefhaus, M. Zangrando, G. De Ninno, G. Lambert, E. Ferrari *et al.*, Phys. Rev. X **4**, 041040 (2014).

[12]T. Mazza, M. Ilchen, A. J. Rafipoor, C. Callegari, P. Finetti, O. Plekan, K. C. Prince, R. Richter, M. B. Danailov, A. Demidovich, L. Avaldi, P. Bolognesi, M. Coreno, P. O'Keeffe, M. Di Fraia, M. Devetta, Y. Ovcharenko, Th. Moeller, V. Lyamayev, F. Stienkemeier, S. Duesterer, K. Ueda, J. T. Costello, A. K. Kazansky, N. M. Kabachnik, M. Meyer *et al.*, Nat. Commun. **5**, 3648 (2014).

[13]T. Wang, D. Zhu, B. Wu, C. Graves, S. Schaffert, T. Rander, L. Müller, B. Vodungbo, C. Baumier, D. P. Bernstein *et al.*, Phys. Rev. Lett. **108**, 267403 (2012).

[14]C. V. Schmising, B. Pfau, M. Schneider, C. M. Gunther, M. Giovannella, J. Perron, B. Vodungbo, L. Mueller, F. Capotondi, E. Pedersoli *et al.*, Phys. Rev. Lett. **112**, 217203 (2014).

[15]C. E. Graves, A. H. Reid, T. Wang, B. Wu, S. de Jong, K. Vahaplar, I. Radu, D. P. Bernstein, M. Messerschmidt, L. Mueller *et al.*, Nat. Mater. **12**, 293 (2013).

[16]A. R. Cameron, P. Riblet, and A. Miller, Phys. Rev. Lett. **76**, 4793–4796 (1996).

[17]G. P. Zhang, W. Hübner, G. Lefkidis, Y. Bai, and T. F. George, Nat. Phys. **5**, 499–502 (2009).

[18]S. P. Weathersby, G. Brown, M. Centurion, T. F. Chase, R. Coffee, J. Corbett, J. P. Eichner, J. C. Frisch, A. R. Fry, M. Gühr *et al.*, Rev. Sci. Instrum. **86**, 073702 (2015).

[19]E. V. Gryzlova, A. N. Grum-Grzhimailo, E. I. Kuzmina, and S. I. Strakhova, J. Phys. B **47**, 19 (2014).

[20]P. Abbamonte, F. Abild-Pedersen, P. Adams, M. Ahmed, F. Albert, R. Alonso Mori, P. Anfinrud, A. Aquila, M. Armstrong, J. Arthur *et al.*, SLAC Report, SLAC-R-1053, 2015.

[21]R. W. Schoenlein, S. Chattopadhyay, H. H. W. Chong, T. E. Glover, P. A. Heimann, C. V. Shank, A. A. Zholents, and M. S. Zolotorev, Science **287**, 2237 (2000).

[22]A. A. Lutman, J. P. MacArthur, M. Ilchen, A. O. Lindahl, J. Buck, R. N. Coffee, G. L. Dakovski, L. Dammann, Y. Ding, H. Dürr *et al.*, Nat. Photonics **10**, 1038 (2016).

[23]R. Sessoli, M. E. Boulon, A. Caneschi, M. Mannini, L. Poggini, F. Wilhelm, and A. Rogalev, Nat. Phys. **11**, 69–74 (2015).

[24]A. K. Kazansky, A. V. Grigorieva, and N. M. Kabachnik, Phys. Rev. Lett. **107**, 253002 (2011).

[25]A. K. Kazansky, A. V. Grigorieva, and N. M. Kabachnik, Phys. Rev. A **85**, 053409 (2012).

[26]J. D. Bozek, Eur. Phys. J.–Spec. Top. **169**, 129 (2009).

[27]E. A. Schneidmiller and M. V. Yurkov, Phys. Rev. Spec. Top.–Accel. Beams **16**, 110702 (2013).

[28]Z. Huang and G. Stupakov, Phys. Rev. Spec. Top.–Accel. Beams **8**, 040702 (2005).

[29]S. Schorb, T. Gorkhover, J. P. Cryan, J. M. Glownia, M. R. Bionta, R. N. Coffee, B. Erk, R. Boll, C. Schmidt, D. Rolles *et al.*, Appl. Phys. Lett. **100**, 121107 (2012).

[30]M. R. Bionta, N. Hartmann, M. Weaver, D. French, D. J. Nicholson, J. P. Cryan, J. M. Glownia, K. Baker, C. Bostedt, M. Chollet *et al.*, Rev. Sci. Instrum. **85**, 083116 (2014).

[31]N. Hartmann, W. Helml, A. Galler, M. R. Bionta, J. Grünert, S. L. Molodtsov, K. R. Ferguson, S. Schorb, M. L. Swiggers, S. Carron *et al.*, Nat. Photonics **8**, 706–709 (2014).

[32]M. Ilchen, L. Glaser, F. Scholz, P. Walter, S. Deinert, A. Rothkirch, J. Seltmann, J. Viefhaus, P. Decleva, B. Langer *et al.*, Phys. Rev. Lett. **112**, 023001 (2014).

[33]V. Schmidt, Rep. Prog. Phys. **55**, 9 (1992).

[34]M. Meyer, J. T. Costello, S. Duesterer, W. B. Li, and P. Radcliffe, J. Phys. B **43**, 194006 (2010).

[35]S. Düsterer, L. Rading, P. Johnsson, A. Rouzee, A. Hundertmark, M. J. J. Vrakking, P. Radcliffe, M. Meyer, A. K. Kazansky, and N. M. Kabachnik, J. Phys. B **46**, 164026 (2013).